Strategies for Dispersing Nanoparticles in Polymers

Ramanan Krishnamoorti

Abstract

Controlling the dispersion of nanoparticles in polymeric matrices is the most significant impediment in the development of high-performance polymer nanocomposite materials and results primarily from the strong interparticle interactions between the nanoparticles. This review examines the theoretical and experimental strategies employed in developing appropriate chemical and physical methods to achieve controlled dispersion of nanoparticles. Methods to characterize the state of dispersion, including force and electron microscopy, and scattering, electrical, and mechanical spectroscopy, are considered with special emphasis on achieving quantitative measures of the dispersion. Some of the outstanding issues, such as long-term aging and the implication for the dispersion of nanoparticles, development of high-throughput methods for rapid screening, and methods for in-line monitoring, are also discussed.

Introduction

The dispersion of nanoparticles in polymeric matrices is the fundamental challenge surrounding the development of polymer nanocomposites. In addition to the development of methods to characterize the dispersions of the nanoparticles (challenged by the multitude of hierarchical length scales), techniques for dispersing aggregated or ordered nanoparticles while not compromising the inherent advantages of the nanoparticles (such as their unique mechanical, thermal, and optical properties and extremely large internal surface area) remain a significant challenge.

The interparticle interactions are clearly a function of the chemical nature of the nanoparticles, with the shape of the nanoparticles, the distance between the nanoparticles, and the polydispersity of particle sizes being the most prominent secondary contributors. Israelachvili has summarized the interaction laws for different particles in vacuum (Table I), and these reveal the strong dependence of the interaction energies on the shape and aspect ratio of the nanoparticles.[1] Further, many nanoparticles form low-dimensional crystals or tight agglomerates that render their dispersion even more difficult. For instance, single-wall carbon nanotubes (SWNTs) have strong van der Waals interactions, resulting in parallel alignment and formation of a triangular lattice with an interaction energy of ~500 eV/μm of nanotube length,[2,3] which is partially responsible for the lack of dispersability of pristine SWNTs. The lack of dispersability of carbon nanotubes is illustrated by considering the concentrations of the nanotubes dispersible in a range of solvents, as shown in Table II.[4] A second example of the strong interactions between nanoparticles is observed in layered silicates, where it has recently been estimated that the cleavage energy for an unmodified montmorillonite is ~133 mJ/m^2, whereas for a similar octadecyl ammonium-modified montmorillonite (where the layers are an additional two nm apart), it is ~40 mJ/m^2, in excellent agreement with experiments.[5] Finally, for chemically identical materials, progressing from spherical nanoparticles (zero-dimensional) to cylindrical nanorods (one-dimensional) to nanoscale-thick sheets (two-dimensional) increases the energy of interaction per pair of nanoparticles and, therefore, increases the complexity of dispersion in a matrix polymer.

Thermodynamic Aspects of Dispersion

Mean-field, self-consistent field (SCF) with field theoretical and simulation methods have been used to understand the dispersion of nanoparticles in solvents and polymeric matrices. The most primitive model for dispersion of stiff rod-like moieties was considered by Onsager[6] and relied exclusively on entropic arguments to indicate that such stiff 1D materials even in the absence of attractive interparticle interactions would undergo an isotropic to nematic transition above a volume fraction that roughly scales as $1/x$, where x is the aspect ratio of the rod. This rather simplistic view captures many of the features associated with the attempted dispersion of carbon and boron nitride nanotubes, wherein extremely limited solubility of these materials is observed in many different small-molecule dispersants.

Vaia and Giannelis[7] have used a simple lattice-based thermodynamic model that examined the entropic and enthalpic contributions during the formation of a polymer layered-silicate nanocomposite to examine the driving forces for intercalation and exfoliation of organically modified layered silicates by long-chain polymers. In their estimation, despite the expected loss of conformational entropy of the confined polymers (even in an exfoliated system, as the free energy calculations are based per unit surface area of the silicate), the gain in conformational entropy of the surfactant tails compensates and leads to the primary conclusion that the enthalpy of the mixing process dominates the free energy considerations. Using the interfacial tension-based formalism of van Oss et al.,[8] Vaia and Giannelis[7] developed an expression for the enthalpy that contains contributions from both van der Waals interactions and polar (Lewis acid/base) interactions. Of these two sets of interaction terms, only the Lewis acid/base term could lead to a favorable enthalpy of mixing; this, combined with the fact that montmorillonite and other layered silicates have a considerable Lewis acid/base contribution, is the dominant thermodynamic driving force for the dispersion of layered silicates in a polymer matrix. This simple lattice-based model provides a straightforward understanding of the structural and chemical changes in the polymer or the surfactant used to functionalize the layered silicates that control dispersion and provides a first understanding of the complex role of thermodynamics in determining the dispersion of nanoparticles in polymers.

Table I: Interaction Laws for Different Particles.[1]

Type of Nanoparticle	van der Waals Interaction Energies
Two spheres (radii, R_1 and R_2) separated by distance D	$W = -\frac{A}{6D}\left(\frac{R_1R_2}{R_1+R_2}\right)$
Two parallel cylinders (radii, R_1 and R_2) separated by a distance D and of length L	$W = -\frac{AL}{12\sqrt{2}D^{3/2}}\left(\frac{R_1R_2}{R_1+R_2}\right)^{1/2}$
Two crossed cylinders (radii, R_1 and R_2) separated by a distance D	$W = -\frac{A}{6D}(R_1R_2)^{1/2}$
Two parallel plates separated by a distance D	$W = -\frac{A}{12\pi D^2}$

Notes: A (Hamaker constant) = $\pi^2C\rho_1\rho_2$, where C is the coefficient in the atom–atom pair potential, and ρ_1 and ρ_2 are the number of atoms per unit volume.

Table II: Room-Temperature Solubilities of Single-Wall Carbon Nanotubes.[4]

Solvent	Solubility in mg L^{-1}
1,2-dichlorobenzene	95
Chloroform	31
1-methylnapthalene	25
1-bromo-2-methylnapthalene	23
N-methylpyrrolidinone	10
Dimethylformamide	7.2
Tetrahydrofuran	4.9
1,2-dimethylbenzene	4.7
Pyridine	4.3
Carbon disulfide	2.6
1,3,5-trimethylbenzene	2.3
Acetone, ethanol, 1,3-dimethylbenzene, 1,4-dimethylbenzene, toluene	<1

A recent model by Mackay et al.[9] has suggested that the dispersion of nanoparticles in a polymer is a result of favorable enthalpy of mixing resulting from the increased molecular contacts between the polymer and the dispersed nanoparticle as compared with the case of aggregated nanoparticles, because of the increased accessible area on the nanoparticle caused by dispersion. Their results indicate that nanoparticles prepared from cross-linked polymers are capable of dispersing in polymers if the size of the nanoparticle is smaller than the radius of gyration of the polymer matrix. The effect, as elucidated by these authors, is only expected in nanoparticles and vanishes at the two limits of extremely small particles as well as for macroscopic particles. It is not readily obvious how these ideas can be extended to the case of nonporous spherical nanoparticles, functionalized spherical nanoparticles, and anisotropic porous and nonporous nanoparticles.

Schweizer and co-workers have used the polymeric reference interaction site model, a theory shown to work excellently to predict the phase behavior of polymer blends, to understand the thermodynamic behavior of nanocomposites comprising flexible polymers and spherical nanoparticles.[10] Miscibility is predicted as a result of a steric stabilization mechanism that results from a small polymer coating strongly adsorbed onto the nanoparticle. Interestingly, they note that the miscibility is relatively independent of polymer molecular weight for weak polymer–nanoparticle interactions, and in the case of strong bridging-induced attraction, an increase in miscibility is observed with increasing molecular weight.

Balazs and co-workers[11,12] have pioneered a method that uses SCF theory based on the theory of Scheutjens and Fleer to calculate the nanoscale interactions and act as input for a density functional theory (DFT), based on the Somoza–Tarazona formulation for anisotropic nanoparticles, that is then used to calculate the equilibrium behavior (phase diagram) of nanocomposites, especially those based on layered silicates. One efficient strategy that they discovered for the dispersion of the clay layers was using mixtures of majority non-functionalized (non-interacting) polymers and a small volume fraction of end-functionalized chains that, depending on the strength of the attractive interaction between the terminal group and the surface, could lead to immiscible, gel-like, and exfoliated structures with increasing attraction between the functionalized polymer and the nanoparticle.

Molecular dynamics (MD) and Monte Carlo simulations were used to understand the dispersion of nanoparticles—especially those of spherical nanoparticles and, to some extent, those of layered silicates and carbon nanotubes. Glotzer and co-workers have examined the mechanism of nanoparticle clustering in a dense non-entangled polymer melt using MD simulations of polyhedral nanoparticles.[13] Their results indicated that the dispersed-to-clustered-state transition was more akin to equilibrium polymerization than a first-order transition such as crystallization. On the other hand, coarse-grained MD simulations of stacks of platelets in a polymer melt indicate that the sliding of the platelets could lead to the breakdown of the platelet stacks; for kinetic reasons, these simulations required the use of non-functionalized (non-attractive) polymers blended with end-functionalized chains.[14] These simulation results are quite similar to the theoretical ones predicted by Ginzburg and Balazs using equilibrium phase diagram calculations based on SCF and DFT methods.[11] Nevertheless, as a result of the hierarchy of length scales and the importance of interparticle and matrix–nanoparticle interactions, it is clear that in order for such simulation methods to play a significant role in the development of dispersion methodologies in polymer nanocomposites, methods such as those employed in multiscale modeling[15] must be incorporated.

Experimental Strategies to Disperse Nanoparticles in Polymeric Matrices

Some of the most prominent methods to achieve dispersion of nanoparticles in polymer matrices have included functionalization of nanoparticles using weak (van der Waals, π-stacking) interactions, ionic interactions, and covalent functionalization. The use of surfactants and polymers interacting with weak forces with nanoparticles has received much attention in dispersing nanoparticles because of significant discoveries in the dispersion of carbon[2] and

boron nitride (BN)[16] nanotubes and, more recently, in the use of nanoemulsions to disperse single nanoparticles. This method clearly preserves many of the attractive properties of the nanoparticles, and in some cases, the stabilizing surfactant or polymers can be removed after dispersion. A good example of this method is the non-covalent supramolecular modification of carbon nanotubes (CNTs) by poly(*m*-phenylenevinylene)-*co*-(2,5-dioctoxy-*p*-phenylenevinylene) (PmPV)–based polymers and starch-based amylose polymers,[17] resulting in CNT dispersion in organic and aqueous solutions, respectively. In the case of the helical amylose, the CNTs are soluble in an aqueous solution of amylose–iodine complex by simultaneous favorable enthalpic interactions and entropy gain as the iodine is released from the complex.[17] Such an entropic–enthalpic combination to achieve dispersion is similar to that observed for many ionic polymers intercalating and exfoliating pristine clays in the presence of water. Recently, PmPV was used to disperse BN nanotubes in chloroform and other organic solvents,[16,18] and it is thought that the mechanism for dispersion is similar to that observed in non-covalent supramolecular modification of CNTs.

On the other hand, for the case of surfactant-assisted stabilization of CNTs, it has been observed that the solubilization occurs for anionic, cationic, and non-ionic surfactants at concentrations significantly lower than the critical micelle concentration. The mechanisms for such dispersion are speculated to be by the formation of rod-like micelles with the nanoparticle embedded at the core of the micelle, the formation of hemi-micelles on the outside of the nanoparticles, and the random adsorption of the surfactants onto the nanotubes. Although direct imaging using electron microscopy appears to be ambiguous regarding the dispersion mechanism, small-angle neutron scattering measurements suggest that random (disordered) adsorption of the surfactant is responsible for the dispersion,[19] and these measurements have been supported recently by computer simulation studies. Regardless of the dispersion mechanism, this use of surfactants and polymers interacting with weak forces with nanoparticles has been a powerful method to disperse nanotubes in solvent and polymeric matrices.

Ionic and covalent functionalization of nanoparticles has been perhaps one of the most extensively studied methods for the dispersion in polymer matrices. For instance, hydroxyl-terminated silica nanoparticles have been treated with organosilanes, and naturally occurring and synthetic layered silicates with hydrated metals populating the interlayer galleries have been ion-exchanged with cationic surfactants with long alkyl or aromatic groups to render them hydrophobic and organophilic. On the other hand, for the case of fullerenes and CNTs, covalent functionalization has proven to be a significant step toward increased solubilization and enhanced compatibility with a range of polymers. The covalent functionalization of CNTs has been reviewed extensively and is not detailed here.[20] The fullerene caps at the ends of the nanotubes are significantly more reactive than the side walls and were initially exploited to attach functional groups. More recently, the development of *in situ* generation and the reaction of organic diazonium compounds with nanotubes in the presence and absence of dispersing solvents and dispersing aids,[21,22] the functionalization by the use of free-radicals,[23] and direct fluorination[24] have enabled and enhanced the possible routes for developing well-dispersed polymer nanocomposites with CNTs.

Aside from the physical mixtures of such functionalized nanoparticles with polymer matrices, two interesting strategies of enhancing dispersion and interactions (physical and mechanical) between the nanoparticle and the matrix are "grafting-to" the nanoparticles with functional polymers and "grafting-from" the nanoparticles with radical, condensation, ring opening, or living or controlled polymerization processes. In fact, one of the pioneering polymer nanocomposites of nylon-6 with layered silicates was developed by the use of ring-opening polymerization with the initiator tethered to the layered silicate by ionic interactions.[25]

The development of controlled radical polymerization methods, such as atom transfer radical polymerization, nitroxide-mediated processes, and degenerative transfer methods, has diversified the range of monomers, functionality, composition, and dimensions of the macromolecules and the derived nanocomposites.[26] The tethering of well-defined polymers to nanoparticles (curved or flat) by grafting-to and grafting-from methods has been successfully demonstrated with thin films of hybrids in which the silica nanoparticles demonstrate a remarkable ordered 2D array, with the interparticle spacing dependent on the size of the tethered polymer chains.[26] Similarly, the grafting of tethered polymers from layered silicates by the use of ionic interactions and controlled polymerization methods has led to an efficient mechanism to ensure dispersion of these nanoparticles in matrices where only demixed or intercalated states were possible using solution and melt processing methods.[27]

Mechanical stresses generated by melt-state shear,[28] ultrasonication in solution,[29,30] and solid-state pulverization[31,32] are extremely effective in the dispersion of aggregated nanoparticles. In particular, ultrasonication has proven extremely popular in the dispersion of CNTs and is one of the few physical methods useful in the dispersion of nanotubes despite the known shortening of the CNTs when subjected to powerful ultrasonication.[30] On the other hand, melt-state processing in conventional polymer processing equipment such as twin-screw extruders results in large shear (and in some cases extension), leading to breakdown of the nanoparticle agglomerates and subsequent individualization and dispersion of the nanoparticles in the polymer matrix. Paul and co-workers[28] have provided an elegant summary of the mechanism for the shear-assisted dispersion of layered silicates in a polymer matrix as shown in Figure 1. This mechanism is similar to the shear-induced breakdown of the superstructure of carbon black and silica commonly observed during the processing of filled rubbers. However, for CNTs no such shear-induced dispersion has been demonstrated, which is perhaps reflective of the strong intertube interaction characteristic of CNTs. Solid-state pulverization at low temperatures provides a novel method to enable dispersion of nanoparticles and has been exploited by Vaia[31] and Torkelson[33] in dispersing layered silicates in polymer matrices. It has also been suggested that this method would be useful for the dispersion of nanotubes, although there is some evidence that suggests that ball milling of CNTs can lead to significant breakdown in the nanotube architecture.[34]

Recently, Schiraldi and co-workers have revived interest in the preparation of aerogels (and xerogels) of nanoparticles and followed it with infiltration by a polymer for the preparation of polymer nanocomposites, thereby avoiding the traditional thermodynamic and kinetic barriers.[35] Extensive work was performed on the development of ultralight, extraordinarily insulating silica aerogel-based polymer nanocomposites where sol-gel processing is combined with guest polymer, monomer, or nanoparticle inclusion followed by supercritical extraction of the solvent.[36] Extending this work, Schiraldi and co-workers[35] exploited freeze-drying of a clay dispersion in deionized water to create a clay aerogel with a density of 0.05 g/cm^3, followed by infiltration by *n*-isopropylacrylamide and subsequent *in situ* polymerization and cross-linking, resulting in a material that was a low-density, thermally responsive hydrogel composite.[35]

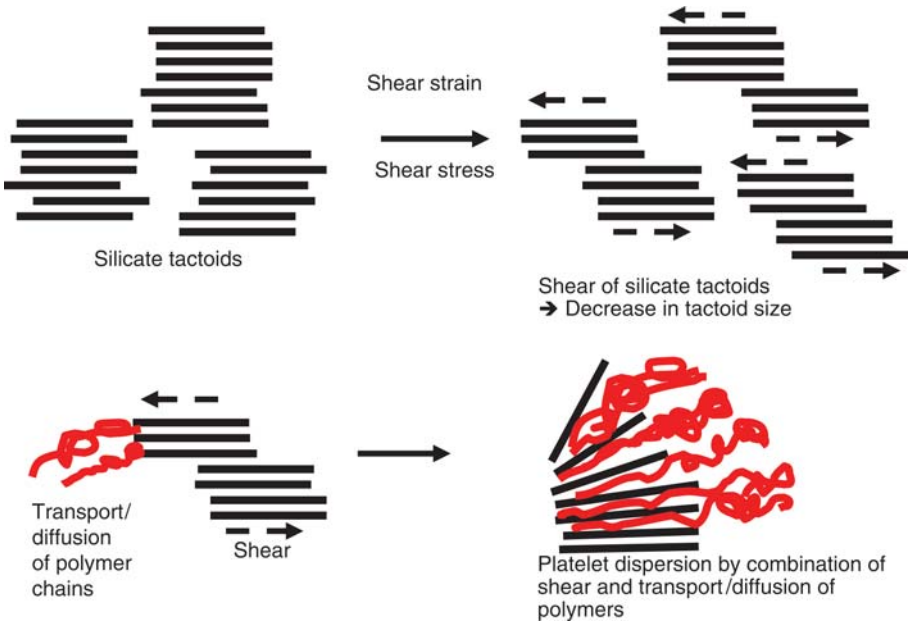

Figure 1. Proposed stepwise process of shear-assisted dispersion of layered silicates in a polymer matrix.[28] Shear is thought to break up the silicate tactoids (micron-sized clusters of silicate aggregates) by a sliding mechanism, consistent with computer simulations.[14] Then, acting in conjunction with the transport/diffusion of the polymer chains, shear enables the dispersion of individual nanometer-thick layers.

Characterization of Dispersion States

The most prominent ways to quantitatively characterize the dispersion state of nanocomposites include microscopy (electron and force), scattering (x-ray, neutron, and light), chemical spectroscopic methods, electrical and dielectric characterization, and mechanical spectroscopy. Although clearly dependent on the details of the nanoparticle, each of these methods can provide unique information on the state of dispersion, ranging from nanometer to micrometer in size scale, and, therefore, they are typically used in combination to provide detailed information on the hierarchical morphology usually present in such nanocomposites.

Electron microscopy has been most extensively used to determine the nanoscale dispersion in different nanocomposites and, in many cases, to qualitatively demonstrate the development of well-dispersed systems. The pioneering work of Gilman, Paul, and Vermogen et al.[37,38] demonstrated the quantitative interpretation of electron micrographs for the case of layered silicate-based nanocomposites by image analysis of several tens of micrographs (Figure 2). This work enabled a direct correlation of the nanoscale dispersion to macroscopic property measurements (mechanical, transport, and flame retardance). Many of these methods have been extended for the use of atomic force microscopy methods in characterizing dispersions of nanotubes and spherical nanodispersions in polymers and require many sets of images and detailed data analysis. Additionally, the development of three-dimensional reconstruction,[39] stereology, and high-resolution transmission electron microscopy and scanning electron microscopy methods[40] have all enabled significant improvements in the understanding of the 3D distribution and dispersion of the nanoparticles.

Radiation scattering and diffraction methods were applied to quantify the dispersion state of the nanoparticles in the matrix.[41] While providing a global (ensemble) average of the dispersion, these methods necessarily require the development of an analytical/numerical model to provide quantitative information regarding the dispersion. X-ray diffraction (XRD) is an invaluable method to provide a first-cut examination of dispersion of layered compounds such as clays and graphene sheets (Figure 3), because of the periodicity of the stacking and the disruption of the stack upon complete dispersion. XRD is also able to provide orientation information in these and multiwall carbon nanotube nanocomposites.[42] Nevertheless, XRD is seldom used as the definitive proof of exfoliation even in those cases, because issues such as surface sensitivity and orientation of the platelets can result in ambiguous results. On the other hand, small-angle x-ray and neutron scattering (SAXS and SANS) have been used to understand the dispersion of nanoparticles such as clays and nanotubes. The extensive SAXS and SANS studies on aqueous dispersions of laponite (a synthetic layered silicate) and montmorillonite, under both static and flow conditions, enabled the generalization of the scattering theory for anisotropic nanoparticles to extract information on the dispersion and alignment of such layered silicates dispersions.[43] These have been extended to the case of organically modified layered silicates in organic solvents by Ho and co-workers using analogies to the analysis of dispersed lamellar block copolymers.[44] Vaia and co-workers further generalized this approach to develop a model that enables the existence of a broad distribution of fully dispersed and stacked platelets (with a distribution of numbers of platelets per stack) and therefore determines quantitatively the extent of dispersion.[45]

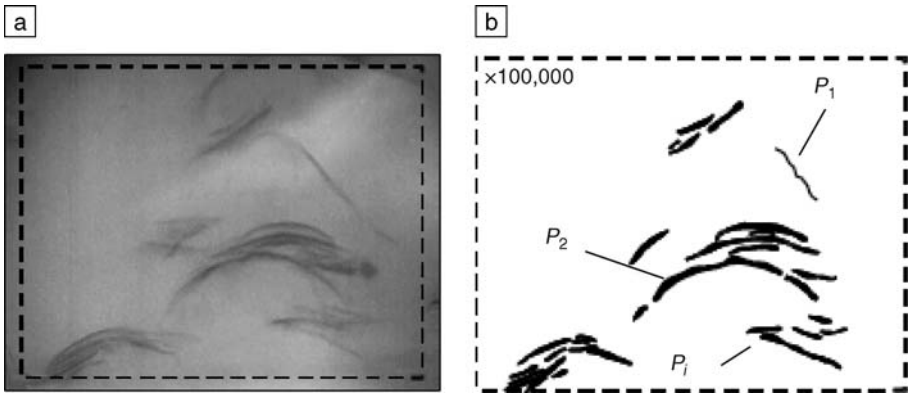

Figure 2. Quantitative analysis of (a) a layered silicate nanocomposite (imaged by transmission electron microscopy) using (b) image analysis methods described by Vermogen et al.[38] to describe the state of clay dispersion. P_i represents the particle number.

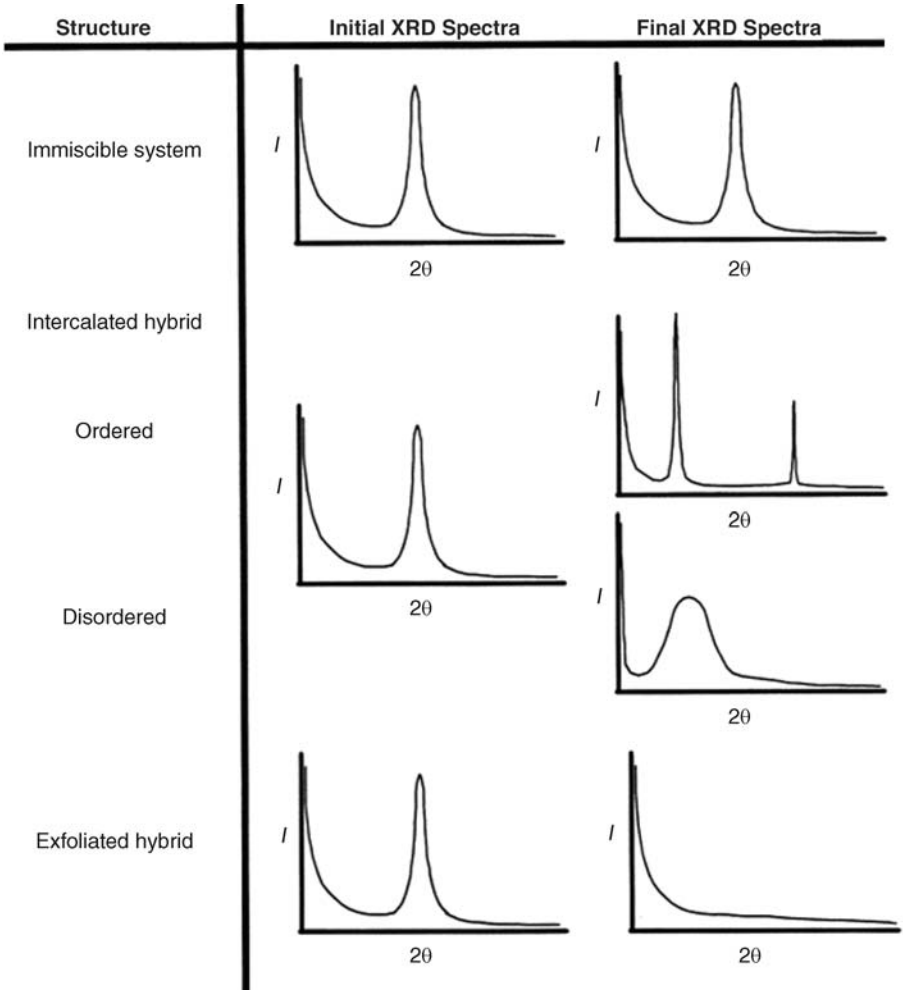

Figure 3. Schematic representation of the angular dependence of the x-ray diffraction (XRD) intensity for different states of dispersion of a layered silicate, from Vaia and Giannelis,[60] indicating the utility of XRD as an initial screening tool in determining the state of nanoparticle dispersion.

On the other hand, quantitatively understanding the dispersion of nanotubes in water, organic solvents, and polymers is still quite primitive.[46] Although it is expected that well-dispersed, non-interacting stiff rods (with length l and diameter d) would exhibit $I(\mathbf{q}) \sim \mathbf{q}^{-1}$ behavior [the scattering vector $\mathbf{q} = 4\pi/\lambda \sin(\theta)$, with λ and θ being the wavelength and half the scattering angle, respectively] for $\mathbf{q}$ values between $2\pi/l$ and $2\pi/d$,[47] there has been limited experimental proof for this scaling relationship.[48] The lack of proof is primarily a result of the low solubilities of CNTs and the uncertainties in guaranteeing well-dispersed and individualized states of the nanotubes in such dispersions.

Alternative measures of the dispersed state of nanoparticles have been sought by the use of chemical spectroscopic tools that are sensitive to local environments and confinement. For instance, Gilman and co-workers used the changes in absorption by organic dye molecules when subjected to changes in interactions and confinement to monitor the state of dispersion of clays in nanocomposites.[49] For the case of nanotubes, Strano and co-workers have demonstrated the use of fluorescence measurements to establish the state of dispersion of the nanotubes.[50]

On the other hand, two powerful macroscopic methods that have yielded significant quantitative measures of the dispersion of nanoparticles in nanocomposites have been mechanical spectroscopy and electrical (and dielectric) characterization. Whereas electrical characterization requires the use of inherently conductive nanoparticles, the rheological analogue to first approximation only requires differences in mechanical character between the matrix and the nanoparticle.[51] Focusing on the melt state (of the polymer or, equivalently, the liquid state of the matrix), a gradual transition from liquid-like to solid-like behavior with increasing nanoparticle concentration is observed in linear viscoelastic studies (Figure 4) and is thought to arise from the development of a geometrically percolated nanoparticle superstructure that exhibits many similarities to jammed and gel-like systems.[22,52–55] On the basis that the onset of solid-like behavior is a result of a geometrical percolation of the nanoparticles, the concentration for this percolation threshold can be used to determine the effective aspect ratio of the nanoparticles in the polymer matrix.[55,56] An important caveat in the use of rheology as a tool to gauge the mesoscale dispersion arises from the observation that such a solid-like response only develops in systems where the interactions between the matrix and the nanoparticles are strong and result in the development of a permanent network.[57]

Outlook

During the last ten years, the scientific and technological methods for dispersing and characterizing dispersions of nanoparticles in polymer matrices has significantly advanced, with the expectation that many of the current developments will lead to the ability to generalize these principles to arbitrary nanoparticles of differing chemical nature, size, shape, and aspect ratio that are becoming readily available as "designer" additives. In addition to the issues outlined here, there are three critical issues that need to be addressed for the successful commercial integration of such materials into materials manufacturing.

The first of these is related to slow "aging" processes during which the structure and properties of the nanocomposites change significantly. Considering the 3D hierarchical nature of the nanocomposites created, the size scale of the well-dispersed nanoparticles that leads them to exhibit both Brownian and non-Brownian dynamics in many cases and the strong and, in some cases, long-range interactions between the nanoparticles render this a crucial scientific issue to be understood. Clearly, accelerated testing methods, well developed for polymeric and polymer composite materials, are well suited to pursue for polymer nanocomposites. However, structural characterization that examines the dispersion and alignment state of nanoparticles must be an integral aspect of such considerations.[58]

The second critical aspect for the development of commercially successful nanocomposites is the integration of high-throughput testing methodologies, which

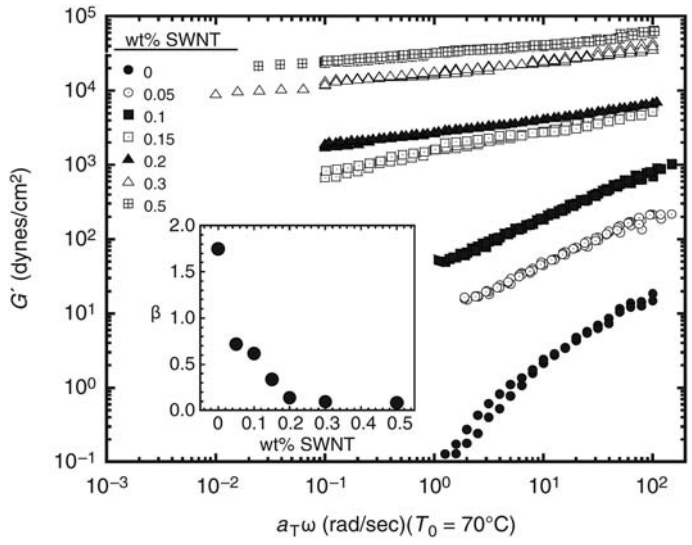

Figure 4. Use of melt-state rheology to demonstrate the development of a solid-like, geometrically percolated network structure. Linear dynamic storage modulus (G') as a function of reduced frequency $a_T\omega$ (where a_T is the temperature-dependent frequency shift factor and ω is the measurement frequency) is compared for different wt% loadings of single-wall carbon nanotubes in poly(ethylene oxide).[54] The low-frequency dependence of G' is described by a power-law dependence, $G' \propto (a_T\omega)^{\beta}$, with the composition dependence of β, the power law exponent, described in the inset of the figure.

dominate materials discovery processes, to probe the state of dispersion with changes in processing and nanoparticle chemistry and correlate with a multitude of mechanical, thermal, and physical properties so as to develop detailed structure–processing–property correlations in a rapid and system-specific manner.

Further, the development of in-line methodologies to provide rapid and sensitive probes to investigate the dispersion of the nanoparticles is crucial for their integration into traditional materials processing. A natural candidate is melt-rheological properties, but extracting dispersion issues from such measurements is complicated, as the rheological signature caused by dispersion is convoluted by changes in the alignment of the nanoparticles.[53] Additional candidates include optical probes such as diffusing wave spectroscopy, infrared, and fluorescence measurements.[49,59] Although there are some issues such as the penetration depth of these probes, they clearly provide a first attempt to address this important issue.

Acknowledgments

Many helpful discussions with Richard Vaia, Evangelos Manias, Sanat Kumar, and Jack Douglas are gratefully acknowledged. Financial support from the Texas Higher Education Coordinating Board through the Advanced Research Program and the Texas Institute for Intelligent Bio-Nano Materials and Structures for Aerospace Vehicles, funded by NASA Cooperative Agreement NCC-1–02038, is gratefully acknowledged.

References

1. J.N. Israelachvili, *Intermolecular Surface Forces* (Academic Press, San Diego, ed. 3, 2006).
2. D.A. Britz, A.N. Khlobystov, *Chem. Soc. Rev.* **35**, 637 (2006).
3. L.A. Girifalco, M. Hodak, R.S. Lee, *Phys. Rev. B* **62**, 13104 (2000).
4. J.L. Bahr, E.T. Mickelson, M.J. Bronikowski, R.E. Smalley, J.M. Tour, *Chem. Commun.,* 193 (2001).
5. H. Heinz, R.A. Vaia, B.L. Farmer, *J. Chem. Phys.* **124**, 224713 (2006).
6. L. Onsager, *Ann. N.Y. Acad. Sci.* **51**, 627 (1949).
7. R.A. Vaia, E.P. Giannelis, *Macromol.* **30**, 7990 (1997).
8. C.J. van Oss, M.K. Chaudhury, R.J. Good, *Chem. Rev.* **88**, 927 (1988)
9. M.E. Mackay et al., *Science* **311**, 1740 (2006).
10. J.B. Hooper, K.S. Schweizer, *Macromol.* **39**, 5133 (2006).
11. V.V. Ginzburg, A.C. Balazs, *Adv. Mater.* **12**, 1805 (2000).
12. A.C. Balazs, C. Singh, E. Zhulina, *Macromol.* **31**, 8370 (1998).
13. F.W. Starr, J.F. Douglas, S.C. Glotzer, *J. Chem. Phys.* **119**, 1777 (2003).
14. K.L. Anderson, A. Sinsawat, R.A. Vaia, B.L. Farmer, *J. Polym. Sci. Part B: Polym. Phys.* **43**, 1014 (2005); A. Sinsawat, K.L. Anderson, R.A. Vaia, B.L. Farmer, *J. Polym. Sci. Part B: Polym. Phys.* **41**, 3272 (2003).
15. N.P. Adhikari et al., *Phys. Rev. Lett.* **93** 188301 (2004).
16. C. Zhi et al., *J. Am. Chem. Soc.* **127**, 15996 (2005).
17. A. Star, D.W. Steuerman, J.R. Heath, J.F. Stoddart, *Angew. Chem. Int. Ed.* **41**, 2508 (2002).
18. C. Zhi et al., *J. Phys. Chem. B* **110**, 1525 (2006).
19. K. Yurekli, C.A. Mitchell, R. Krishnamoorti, *J. Am. Chem. Soc.* **126**, 9902 (2004).
20. A. Hirsch, O. Vostrowsky, *Funct. Mol. Struct.* **245**, 193 (2005).
21. J.L. Bahr, J.M. Tour, *Chem. Mater.* **13**, 3823 (2001); C.A. Dyke, J.M. Tour, *J. Phys. Chem. A* **108**, 11151 (2004).
22. C.A. Mitchell et al., *Macromol.* **35**, 8825 (2002).
23. Y.M. Ying et al., *Org. Lett.* **5**, 1471 (2003).
24. V.N. Khabashesku, W.E. Billups, J.L. Margrave, *Acc. Chem. Res.* **35**, 1087 (2002).
25. A. Usuki et al., *J. Mater. Res.* **8**, 1179 (1993).
26. J. Pyun, K. Matyjaszewski, *Chem. Mater.* **13**, 3436 (2001).
27. Z.M. Wang, H. Nakajima, E. Manias, T.C. Chung, *Macromol.* **36**, 8919 (2003); L. Xu et al., *Nanotechnology* **16**, S514 (2005).
28. T.D. Fornes, P.J. Yoon, H. Keskkula, D.R. Paul, *Polym.* **42**, 9929 (2001).
29. J. Zhao, A.B. Morgan, J.D. Harris, *Polym.* **46**, 8641 (2005).
30. C. Park et al., *Chem. Phys. Lett.* **364**, 303 (2002).
31. H. Koerner, D. Misra, A. Tan, L. Drummy, P. Mirau, R. Vaia, *Polymer* **47**, 3426 (2006).
32. K. Khait, J.M. Torkelson, *Polym. Plast. Technol. Eng.* **38**, 445 (1999).
33. J.M. Torkelson, A. Lebovitz, K. Kasimatis, K. Khait, "Method of producing exfoliated polymer-clay nanocomposite and polymer-clay nanocomposite produced therefrom," U.S. Patent Application No. 20060178465 (August 10, 2006).
34. N. Pierard et al., *Carbon* **42**, 1691 (2004).
35. S. Bandi, M. Bell, D.A. Schiraldi, *Macromol.* **38**, 9216 (2005).
36. L.A. Capadona, M.A.B. Meador, A. Alunni, E.F. Fabrizio, P. Vassilaras, N. Leventis, *Polymer* **47**, 5754 (2006); P. Innocenzi, G. Brusatin, *Chem. Mater.* **13**, 3126 (2001).
37. A.B. Morgan, J.W. Gilman, *J. Appl. Polym. Sci.* **87**, 1329 (2003); T.D. Fornes et al., *Polym.* **43**, 5915 (2002); H.R. Dennis et al., *Polym.* **42**, 9513 (2001).
38. A. Vermogen et al., *Macromol.* **38**, 9661 (2005).
39. A. Usuki, N. Hasegawa, H. Kadoura, T. Okamoto, *Nano Lett.* **1**, 271 (2001); E. Kumacheva, O.K.L. Lilge, *Adv. Mater.* **11**, 231 (1999).
40. L.F. Drummy et al., *J. Phys. Chem. B* **109**, 17868 (2005); J. Ryszkowska, in *Adv. Mater. Forum III, Pts. 1–2,* **514–516**, 1658 (2006); Z.L. Wang, *Adv. Mater.* **15**, 1497 (2003).
41. D.W. Schaefer, M.M. Agamalian, *Curr. Opin. Solid State Mater. Sci.* **8**, 39 (2004); B.J. Olivier et al., *Macromol.* **29**, 8615 (1996).
42. M. Gelfer et al., *Langmuir* **20**, 3746 (2004); A. Bafna, G. Beaucage, F. Mirabella, S. Mehta, *Polymer* **44**, 1103 (2003).
43. J.D.F. Ramsay, P. Lindner, *J. Chem. Soc. Faraday Trans.* **89**, 4207 (1993); J.D.F. Ramsay, S.W. Swanton, J. Bunce, *J. Chem. Soc. Faraday Trans.* **86**, 3919 (1990).
44. D.L. Ho, R.M. Briber, C.J. Glinka, *Chem. Mater.* **13**, 1923 (2001).
45. R.A. Vaia, W.D. Liu, H. Koerner, *J. Polym. Sci. Part B: Polym. Phys.* **41,** 3214 (2003).
46. D.W. Schaefer et al., *Chem. Phys. Lett.* **375**, 369 (2003).
47. M. Moniruzzaman, K.I. Winey, *Macromol.* **39**, 5194 (2006).

48. W. Zhou et al., *Chem. Phys. Lett.* **384**, 185 (2004).
49. P.H. Maupin, J.W. Gilman, R.H. Harris, S. Bellayer, A.J. Bur, S.C. Roth, M. Murariu, A.B. Morgan, J.D. Harris, *Macromol. Rapid Commun.* **25**, 788 (2004).
50. R.A. Graff et al., *Adv. Mater.* **17**, 980 (2005).
51. C. Park et al., *J. Polym. Sci. Part B: Polym. Phys.* **44**, 1751 (2006).
52. M. Surve, V. Pryamitsyn, V. Ganesan, *Langmuir* **22**, 969 (2006).
53. R. Krishnamoorti, K. Yurekli, *Curr. Opin. Colloid Interface Sci.* **6**, 464 (2001).
54. T. Chatterjee, K. Yurekli, V.G. Hadjiev, R. Krishnamoorti, *Adv. Funct. Mater.* **15**, 1832 (2005).
55. J. Ren, A.S. Silva, R. Krishnamoorti, *Macromolecules* **33**, 3739 (2000).
56. E.J. Garboczi, K.A. Snyder, J.F. Douglas, M.F. Thorpe, *Phys. Rev. E* **52**, 819 (1995).
57. S. Salaniwal, S.K. Kumar, J.F. Douglas, *Phys. Rev. Lett.* **89**, 258301 (2002); G. Schmidt et al., *Macromolecules* **33**, 7219 (2000); C.A. Mitchell, R. Krishnamoorti, *Macromolecules* **40**, 1538 (2007).
58. J.X. Ren, B.F. Casanueva, C.A. Mitchell, R. Krishnamoorti, *Macromolecules* **36**, 4188 (2003); V. Goel et al., *J. Polym. Sci. Part B: Polym. Phys.* **44**, 2014 (2006).
59. D.A. Tsyboulski, S.M. Bachilo, R.B. Weisman, *Nano Lett.* **5**, 975 (2005).
60. R.A. Vaia, E.P. Giannelis, *Macromolecules* **30**, 8000 (1997). □